

## Immobilization of Cr (VI) in Bagasse Ash Blended Cement Pastes

A. M. El-Roudi, M. A. Tantawy<sup>#</sup> and A. A. Salem

Chemistry Department, Faculty of Science, Minia University,  
Minia, Egypt.

**T**HE OBJECTIVE of this study is to investigate the possibility of utilizing bagasse ash to improve the cement immobilization of chromium (VI). It was concluded that the blended cement which contain 15-20% bagasse ash can be used effectively for immobilization of concentrated waste Cr (VI) solutions ( $\approx 13000$  ppm Cr (VI)) after being mixed with the blended cement in water to cement ratio of about 30%. The immobilized cement paste will set at about 4hr and gain satisfactory compressive strength of about  $450 \text{ kg/cm}^2$ . The immobilization efficiency  $\approx 90\%$  under this conditions.

**Keywords:** Bagasse ash, Blended cement, Pozzolana, Cement immobilization and Cr (VI).

Chromium is one of the heavy metals that has both beneficial and detrimental properties and is generated from many industrial processes such as electroplating, leather tanning, paints and pigments, textile, steel fabrication and production of chromium chemicals. Chromium usually exists in its compounds in the forms of trivalent chromium [Cr (III)] and hexavalent chromium [Cr (VI)] in the environment. The later is the most important one because of its toxicity, solubility, mobility characteristics, strong oxidizing and carcinogenic nature <sup>(1-3)</sup>. In recent years, large quantity of Cr (VI) containing wastes that lead to serious environmental problems and hazardous risks are discharged into the environment. Chromium contamination up to  $130,000 \text{ mg/kg}$  has been reported <sup>(1,4)</sup>. Cement-based solidification–stabilization (S/S) treatment technology combines two interrelated processes that occur simultaneously to produce a material that will have reduced environmental impact when disposed or reused. Solidification process involves encapsulation of the waste within a solid cementitious matrix to produce a solid product with improved physical properties, primarily strength. Stabilization process involves binding of the compounds of a hazardous waste stream into a stable insoluble less mobile and less toxic form since the solubility of many pollutants is severely reduced by the high pH environment within a cement paste <sup>(5)</sup>. The US Environmental Protection Agency (EPA) has identified S/S as the best demonstrated available technology for 57 listed hazardous wastes <sup>(6)</sup>.

---

<sup>#</sup>Corresponding author, E-mail: [matantawy75@yahoo.com](mailto:matantawy75@yahoo.com).

Bagasse ash is the waste generated by the combustion of bagasse. Apart from silica which is the major component, it contains other metal oxides as well as unburned carbon<sup>(7)</sup>. Around 0.005-0.066 tons ash is generated per ton of sugarcane crushed<sup>(8)</sup>. This waste is typically disposed off in pits, it is also applied on land for soil amendment. In Egypt, there are more than 12 sugar refinery plants producing huge amounts of bagasse ash annually. Limited portion of these wastes has been recycled primarily as soil amendment. However, the rest of bagasse ash due to its abundance is useless and currently being disposed to open landfills causing serious environmental impact. Bagasse ash used as an additive for production of building bricks<sup>(9)</sup> and as a cement replacement<sup>(10)</sup>. Bagasse ash was found to improve the mechanical properties of cement mortar<sup>(11)</sup>, normal concrete<sup>(12)</sup>, self compacting concrete<sup>(13)</sup> as well as conventional hollow concrete<sup>(14)</sup>. Bagasse ash also was found to improve the durability of concrete under aggressive environment<sup>(15)</sup>. The use of bagasse ash as a cement replacement for immobilization of heavy metals not only marks a novelty in the immobilization technology but also assists in alleviating disposal problem of bagasse ash heaps in Egypt.

Many investigators have analyzed the effect of Cr (III) and (VI) on the different Portland cement phases<sup>(16-18)</sup> and its solidification in cementitious matrix<sup>(19-21)</sup>. Immobilization of chromium affects the pore formation mechanism causing a wide variety of pore diameters to appear (with the small 0.01 $\mu$ m diameter pores dominating) indicating involvement of chromium in silicate formation in the C-S-H matrix<sup>(22,23)</sup>. The addition of Cr (VI) may retard hydration reactions<sup>(24, 25)</sup> as a result of the reduction in permeability caused by precipitation of calcium chromate and coating on cement grain surfaces<sup>(26, 27)</sup>. The addition of Cr (VI) increased the setting times of cement, inhibits cement hydration and reduced the compressive strength of the solidified cement<sup>(2)</sup>. The addition of Cr (VI) increased the setting times of cement and impairs the strength development of marble dust blended cement<sup>(28)</sup>. The addition of Cr (VI) retards the hydration and reduces the compressive strength of limestone blended cement especially at early ages<sup>(21)</sup>. The accelerating effect of some chromium compounds (chromates, chromium chloride, nitrate) on the reaction of the main cement phases with water is known<sup>(29,30)</sup>. The addition of Cr (VI) may accelerate hydration reactions without significant changes in the hydration mechanism<sup>(31)</sup>. This effect is explained by precipitation of calcium chromate and the increased demand for Ca<sup>2+</sup> ions in the cement pore solution. As a result, unhydrated cement fractions satisfies the increased demand of Ca<sup>2+</sup> ions and accelerates hydration of C<sub>3</sub>S<sup>(32, 33)</sup>.

It was found that immobilization of Cr (III) in cement paste is excellent regardless of the type of cement due to the Cr(OH)<sub>3</sub> precipitation mechanism while that of Cr (VI) depends on the type of cement because Cr (VI) occurs in the form of relatively soluble chromates<sup>(34)</sup>. The mechanism of Cr (VI) immobilization in cement paste is not fully explained<sup>(35, 36)</sup>. Most treatment methods have failed to reduce the leaching of Cr (VI) to meet the toxicity characteristics leaching procedures (TCLP) extraction limit of less than 5 ppm because of the complexity of chromium chemistry<sup>(37, 38)</sup>.

During cement immobilization of chromate, the moderately oxidizing environment provided by cement preserves chromium in form of chromate (oxidized state, Cr (VI)) rather than chromium ion (reduced state, Cr (III)). The high pH of the pore solution of hydrated cement paste may result in formation of poorly ordered structures of calcium chromate precipitate  $\text{Ca}_2\text{CrO}_5 \cdot 3\text{H}_2\text{O}$  (detected by XRD) or formation of amorphous structures in cement pastes<sup>(33, 39)</sup> (not be detected by XRD). Physical adsorption of chromate ions may occur due to attraction of chromate ions in the pore solution to the surfaces of cementitious products of unsatisfied surface charges. Chemical adsorption of chromate ions may occur due to affinity and specific adsorption of cementitious products to chromate ions<sup>(40, 41)</sup>. Occlusion or encapsulation of chromate ions in the lattice structures of C-S-H may occur during precipitation of cement hydration products<sup>(42, 43)</sup> altering their crystallinity, particle size and solubility<sup>(44)</sup>. Calcium chromate precipitate may be incorporated in the tetrahedral silicate sites in the C-S-H matrix<sup>(45)</sup>.

The formation of modified Cr-ettringite,  $3\text{CaO} \cdot \text{Al}_2\text{O}_3 \cdot 3\text{CaCrO}_4 \cdot 32\text{H}_2\text{O}$ ,<sup>(46-48)</sup> which may occur due to substitution of  $\text{SO}_4^{2-}$  in ettringite structure by  $\text{CrO}_4^{2-}$ <sup>(49)</sup> is one possible mechanism involved in immobilization of chromate in cement. However, this mechanism may require a high concentration of chromate ions present in pore solution, being in equilibrium with solid. Also, the immobilization of chromate can be related to the formation of Ca-Cr aluminates and the formation of phases such as  $\text{Ca}_4\text{Al}_6\text{O}_{12}\text{CrO}_4$  and  $\text{Ca}_6\text{Al}_4\text{Cr}_2\text{O}_5$ <sup>(16, 17)</sup>. It was reported that at elevated pH (approximately 12.8), the formation of calcium aluminosilicate hydrates CAS and CSH is mainly responsible for Cr (VI) immobilization based on the use of quicklime and fly ash through surface sorption, inclusion and physical entrapment<sup>(50)</sup> or through the formation of pozzolanic compound  $3\text{CaOAl}_2\text{O}_3 \cdot 0.5\text{CaCrO}_4 \cdot 0.5\text{CaSO}_4 \cdot n\text{H}_2\text{O}$ <sup>(51-53)</sup>.

It was found that the mechanism by which Cr (VI) is bound to cementitious matrix influences the leaching mechanism<sup>(54)</sup>. The leachability of Cr (VI) from solidified cement mixtures depends on the initial Cr (VI) concentration and the leaching time<sup>(2)</sup>. The leachability of Cr (VI) in fly ash cement mortars greatly depends on leachant pH, carbonation of cement mortars increases the leaching of chromium ions and addition of ground granulated blast furnace slag decreases the leaching of Cr (VI) from solidified fly ashes<sup>(55)</sup>. The cement immobilization of Cr (VI) improved by blending cement with limestone<sup>(21)</sup> and marble dust<sup>(28)</sup>. The incorporation of polycarboxylate-based superplasticizer was found to decrease the leaching of Cr (VI) significantly during cement immobilization of chromium residue generated from chromate plant and metallic chromium production. Sodium and organophilic bentonite were found to improve the immobilization of tannery waste containing chromium using Portland cement type II and the best treatment conditions are obtained when both additives are used<sup>(56)</sup>.

### Materials and Experimental

The raw materials used in this work are OPC [CEM I (No.42.5)] and sugar cane bagasse ash. OPC purchased from Beni-Suif Cement Co., Egypt. The sugar cane bagasse ash sample used in this study was collected from the boiler of nearby sugar factory in Minia Governorate, Egypt. According to previous study<sup>(57)</sup> it was found that the optimum calcination condition that enhances the pozzolanic activity of bagasse ash is 700-800°C for 3 hr. Calcination of bagasse ash was carried out in an electrical muffle furnace with a heating rate 10 °C/min at 700°C for 3 hr. then recharged from the muffle furnace and cooled to room temperature in desiccator. To avoid any possible influence of the fineness of the calcined samples, calcined bagasse ash was ground to pass 90 µm sieve. An analytical grade K<sub>2</sub>CrO<sub>4</sub> (Aldrich Co.) was prepared and used to investigate the cement immobilization of Cr (VI). 5 % K<sub>2</sub>CrO<sub>4</sub> solution (wt/volume) was prepared (13000 ppm of Cr (VI)) in distilled water. Six mixes were prepared by replacement of OPC with 10-25 % bagasse ash. The mix composition of blended cements is shown in Table 1.

**TABLE 1. Mix composition in wt % of bagasse ash blended.**

Symbol	OPC	Bagasse ash
C	100	0
B1	90	10
B2	85	15
B3	80	20
B4	75	25

The water of normal consistency and the initial as well as final setting times were determined using Vicat apparatus according to ASTM Designations C 187-98 and C 191-01a , respectively<sup>(58, 59)</sup> . Mixing of dry cement mixes was carried out using the required water of standard consistency. In case of immobilization of Cr (VI) in cement, before mixing, 60 ml of 5% K<sub>2</sub>CrO<sub>4</sub> solution were completed to the same water to solid ratio as in the hydration step and added to 220 g blended cement. Hence ratio of Cr (VI) 0.36% or 1.36% as K<sub>2</sub>CrO<sub>4</sub> were used, by weight of solid binder. Moulding of the cement pastes was carried out in stainless steel (2 × 2 × 2 cm) mould. Immediately after moulding, blended cement pastes were cured at about 100 % relative humidity, demolded after 24hr and cured for 28 and 90 days in closed humidity chamber without mixing of hydrated cubes with water to avoid leaching of chromium. Bulk density was determined using Archimedes principle<sup>(60)</sup> .

The compressive strength measurement was carried out using a manual compressive strength machine using set of three cubes according to ASTM Designation C 109-80<sup>(61)</sup> . Determination of free water content is carried out by microwave technique using domestic microwave oven (Olympic electric model

KOR-131G, 2450 MHz, 1000 W) <sup>(62)</sup>. The determination of combined water content (Wn) was carried out using samples of hydration stopped specimen after ignition in porcelain crucibles at 1000°C for 1 hr in a muffle furnace and cooling in a desiccator. The total porosity of the hardened cement paste is calculated according to Copeland and Hayes<sup>(63)</sup>. The Cr immobilization efficiency after 28 and 90 days of hydration was carried out in accordance with the standard procedures prescribed by the United States Environmental Protection Agency, toxicity characteristic leaching procedure (TCLP) method 1311 <sup>(64)</sup>. Cr (VI) concentration of the leachate was determined using Perkin-Elmer Lambda 35 UV/VIS Spectrometer using diphenylcarbazide <sup>(65)</sup>.

The X-ray diffraction (XRD) analysis was carried out with the aid of Philips X-ray diffractometer PW 1370, Co. using Ni filtered CuK<sub>α</sub> radiation (1.5406 Å) under 30 kV operating voltage and 24 mA emission current. The step-scan covered the angular range 15-60° (2θ). The Mineralogical composition of the investigated samples was identified by the aid of the PDF standards. The X-ray fluorescence (XRF) analysis was carried out by the same apparatus. The thermogravimetric analysis (TGA) was carried out with the aid of Shimadzu Corporation thermo analyzer with DTG-60H detector. About 5 mg of finely powdered sample was put in an aluminium cell and heated with 10 °C/min heating rate, under nitrogen atmosphere at 40 ml/min flow rate, the hold time at the appropriate temperature is zero. The Fourier transform infrared (FTIR) spectra were measured by the spectrometer Perkin Elmer FTIR system Spectrum X. Samples were prepared by mixing 1 mg of the sample in 200 mg of KBr. The spectral analysis was performed in the range 400-4000 cm<sup>-1</sup> with spectral resolution of 1 cm<sup>-1</sup>. Scanning electron microscopy (SEM) was investigated by the aid of Jeol-Dsm 5400 LG apparatus to examine the morphology and microstructure of selected samples by mounting on stubs and coating with gold prior to analysis to make them electrically conductive.

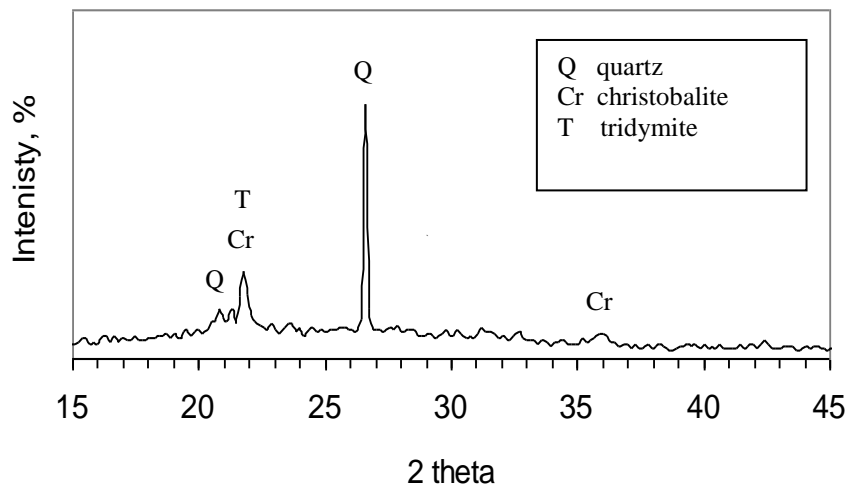
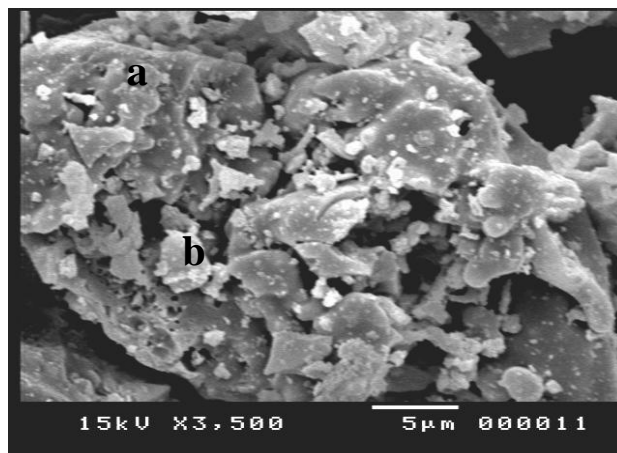
## Results and Discussion

### *Characterization of raw materials*

The chemical composition of the OPC and bagasse ash calcined at 700°C for 3 hr determined by XRF analysis is shown in Table 2. The chemical composition of bagasse ash illustrates that bagasse ash contains high amount of SiO<sub>2</sub> (75.23 wt %) in addition to small amounts of CaO, Fe<sub>2</sub>O<sub>3</sub>, Al<sub>2</sub>O<sub>3</sub>, MgO, Na<sub>2</sub>O and K<sub>2</sub>O. The sum of SiO<sub>2</sub>, Al<sub>2</sub>O<sub>3</sub> and Fe<sub>2</sub>O<sub>3</sub> equals to 85.89 wt % which is in good agreement with the requirements (>70 wt %) stated in ASTM designation: C 618-89 <sup>(66)</sup> for natural pozzolana. The phase composition of OPC, wt % according to Bouge's calculations is ; 47.78% C<sub>3</sub>S, 23.83% β-C<sub>2</sub>S, 10.73% C<sub>3</sub>A, 9.68% C<sub>4</sub>AF and 0.914% LSF. Figure 1 is the XRD patterns of bagasse ash calcined at 700°C for 3 hr and illustrates that bagasse ash contains amorphous silica as indicated from the heap in the range 15-35 2θ in addition to quartz, tridymite and cristobalite. Figure 2 is the SEM micrograph of bagasse ash calcined at 700 for 3hr and illustrates that silica aggregate may appear as dark grains (a) and residues may appear as white small particles (b).

**TABLE 2. Chemical composition wt % of OPC and bagasse ash.**

Material	SiO <sub>2</sub>	Al <sub>2</sub> O <sub>3</sub>	Fe <sub>2</sub> O <sub>3</sub>	CaO	MgO	SO <sub>3</sub>	Na <sub>2</sub> O	K <sub>2</sub> O	L.O.I	Total
OPC	20.88	6.08	3.18	63.00	1.50	1.60	0.22	0.24	2.35	99.05
Bagasse ash	50.69	13.56	11.78	10.57	4.24	0.04	3.06	0.49	4.41	98.84

**Fig. 1. The XRD patterns of bagasse ash calcined at 700°C for 3 hr.****Fig. 2. SEM micrograph of bagasse ash calcinated at 700 °C for 3hr.**

*Hydration characteristics of blended cement pastes*

Figure 3 illustrates the water of consistency, initial and final setting times of bagasse ash blended cement pastes. The water of consistency increases linearly with bagasse ash content may be due to that bagasse ash markedly increases the amount of surface water which related to the specific surface of the system <sup>(67)</sup>. The setting time elongates with bagasse ash content may be due to increasing the amount of mixing water <sup>(68)</sup> as well as decreasing clinker content which has shorter setting time <sup>(69)</sup>. The elongation of setting time also may be due to the formation of a layer of bagasse ash particles around anhydrous cement grains which delays the hydration of C<sub>3</sub>S. The thickness of this layer increases with bagasse ash content hence the rate of hydration of cement decreases <sup>(70)</sup> (Table 3).

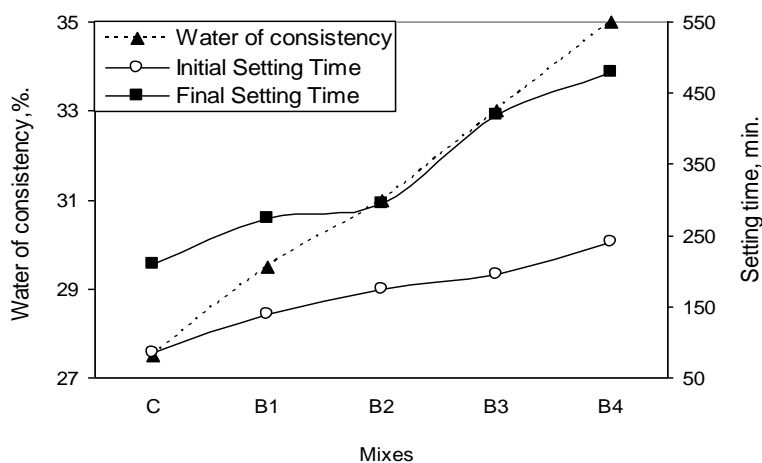


**Fig.3.** The water of consistency, initial and final setting times of bagasse ash blended cement pastes.

**TABLE 3.** The water of consistency, initial and final setting times of bagasse ash blended cement pastes.

Sample	Water of consistency, %	Initial setting time, min	Final setting time, min
C	27.5	85	210
B1	29.5	140	275
B2	31	175	295
B3	33	195	420
B4	35	240	480

Figure 4 and Table 4 represent the combined water content of bagasse ash blended cement pastes hydrated up to 90 days. The combined water content decreases with bagasse ash content may be due to that bagasse ash at lower substitution level acts as a nucleating agent for hydration products enhancing the cement hydration while increasing bagasse ash content makes a dilution effect.

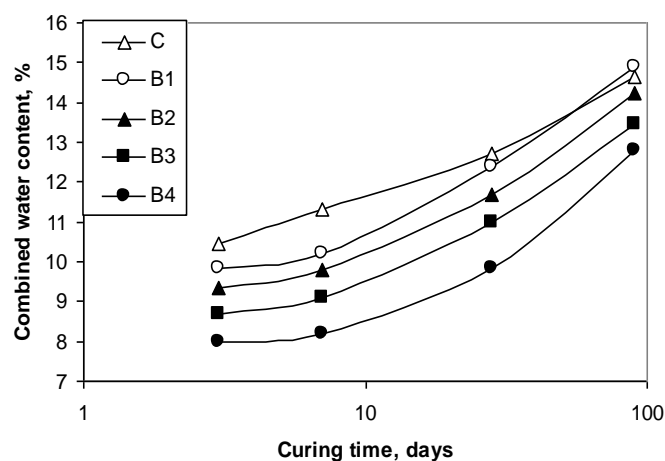


Fig. 4. The combined water content of bagasse ash blended cement pastent hydrat.

TABLE 4. The combined water content of bagasse ash blended cement pastes hydrated up to 90 days.

Sample	Combined water content, %			
	3 days	7 days	28 days	90 days
C	10.44	11.30	12.72	14.65
B1	9.82	10.20	12.37	14.89
B2	9.34	9.80	11.67	14.22
B3	8.67	9.10	11.00	13.45
B4	7.98	8.20	9.84	12.78

Figure 5 and Table 5 represent the bulk density and total porosity of bagasse ash blended cement pastes hydrated up to 90 days. The bulk density decreases while the total porosity increases with bagasse ash content due to the dilution effect of bagasse ash by reducing the amount of OPC, hence the amount of hydration product reduced and as a result the bulk density decreases and the total porosity increases. The bulk density decreases with bagasse ash content may also be due to that bagasse ash have lower specific gravity than OPC.



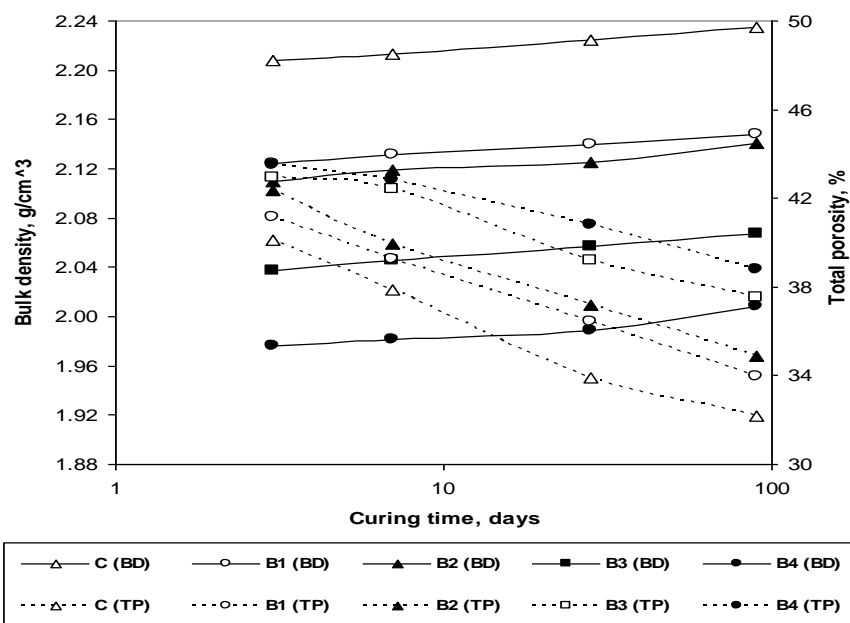


Fig. 5. The bulk density and total porosity of bagasse ash blended cement pastes hydrated up to 90 days.

TABLE 5. The bulk density and total porosity of bagasse ash blended cement pastes hydrated up to 90 days.

Sample	Bulk density, g/cm <sup>3</sup>			
	3 days	7 days	28 days	90 days
C	2.2083	2.2132	2.2248	2.2350
B1	2.1240	2.1316	2.1401	2.1475
B2	2.1101	2.1191	2.1248	2.1407
B3	2.0368	2.0452	2.0568	2.0668
B4	1.9759	1.9811	1.9886	2.0080
Sample	Total porosity, %			
	3 days	7 days	28 days	90 days
C	40.12	37.90	33.91	32.16
B1	41.15	39.25	36.43	33.97
B2	42.37	39.97	37.16	34.90
B3	42.91	42.39	39.22	37.55
B4	43.51	42.81	40.81	38.77

Figure 6 and Table 6 show the compressive strength of bagasse ash blended cement pastes hydrated up to 90 days. Blended cement pastes have low compressive strength at early ages of hydration then the rate of strength development enhanced at later ages. Bagasse ash at the early ages of hydration acts as a filler then at later ages of hydration it acts as pozzolana and reacts with portlandite CH (accumulated in the pore of hydrated cement pastes as a result of hydration of clinker phases) giving additional calcium silicate hydrates. The compressive strength decreases with bagasse ash content because of the dilution of hydrated cement pastes by decreasing the OPC content.

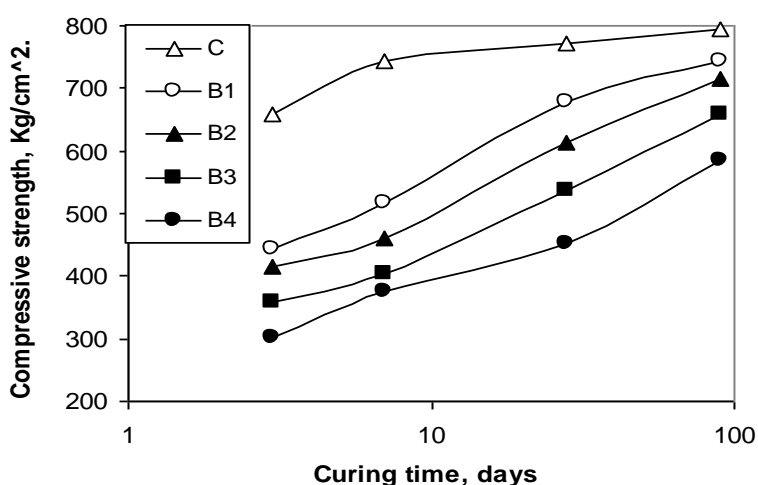
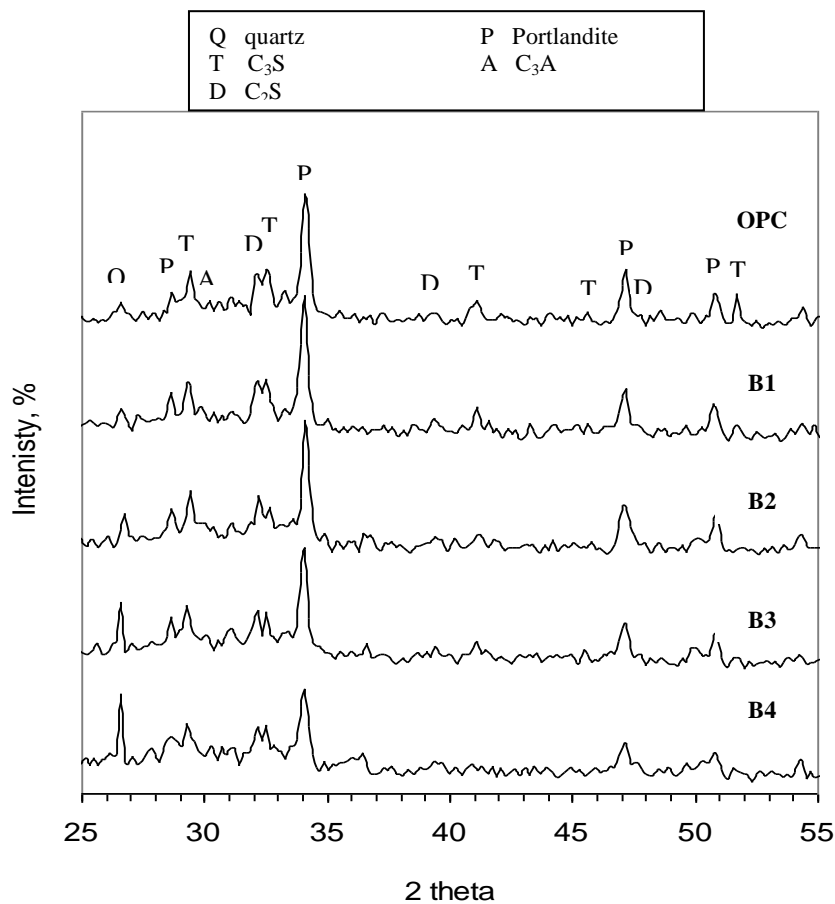


Fig. 6. The compressive strength of bagasse ash blended cement pastes hydrated up to 90 days.

TABLE 6. The compressive strength of bagasse ash blended cement pastes hydrated up to 90 days.

Sample	Compressive strength, Kg/cm <sup>2</sup>			
	3 days	7 days	28 days	90 days
C	659	744	772	794
B1	443	518	678	744
B2	414	461	612	716
B3	358	405	537	659
B4	301	377	452	584

Figure 7 illustrates the XRD patterns of bagasse ash blended cement pastes hydrated for 90 days. The amount of unhydrated clinker phases  $C_2S$  and  $C_3S$  decreases with bagasse ash content because of dilution of cement by bagasse ash and due to that bagasse activates the hydration of cement. Portlandite decreases also with bagasse content because of the previous reasons in addition to pozzolanic activity of bagasse ash which consumes portlandite forming additional C-S-H.



**Fig.7.**The XRD patterns of bagasse ash blended cement pastes hydrated for 90 days.

Figure 8 illustrates the FTIR patterns of bagasse ash blended cements hydrated for 90 days. The absorption bands of carbonate increase with bagasse ash content may be attributed to that total porosity of hydrated cement pastes

increase with bagasse ash content, which in turn increases the rate of carbonation of hydrated cement pastes. The absorption band of C-S-H at  $978\text{ cm}^{-1}$  (stretching vibration  $\nu_3$  of  $\text{SiO}_4^{4-}$ ) shifts to higher wavenumber values with increasing bagasse ash content. This may be due to that C-S-H formed by the pozzolanic action of bagasse ash differs (in its nature and water content) from that formed by hydration of OPC. The absorption band of silica which appeared at  $462\text{ cm}^{-1}$  corresponding to bending vibration of O-Si-O arises from the replacement of OPC with bagasse ash. The ettringite band at  $1124\text{ cm}^{-1}$  disappeared due to that  $\text{SO}_4^{2-}$  ions were probably replaced by  $\text{CO}_3^{2-}$  ions in case of bagasse ash blended cement pastes. The absorption band observed at  $3640\text{ cm}^{-1}$  which is due to O-H stretching of  $\text{Ca(OH)}_2$  increases at high bagasse ash content. This may be attributed to that bagasse ash has a low pozzolanic activity because higher amount of portlandite accumulated despite the dilution effect of bagasse ash.

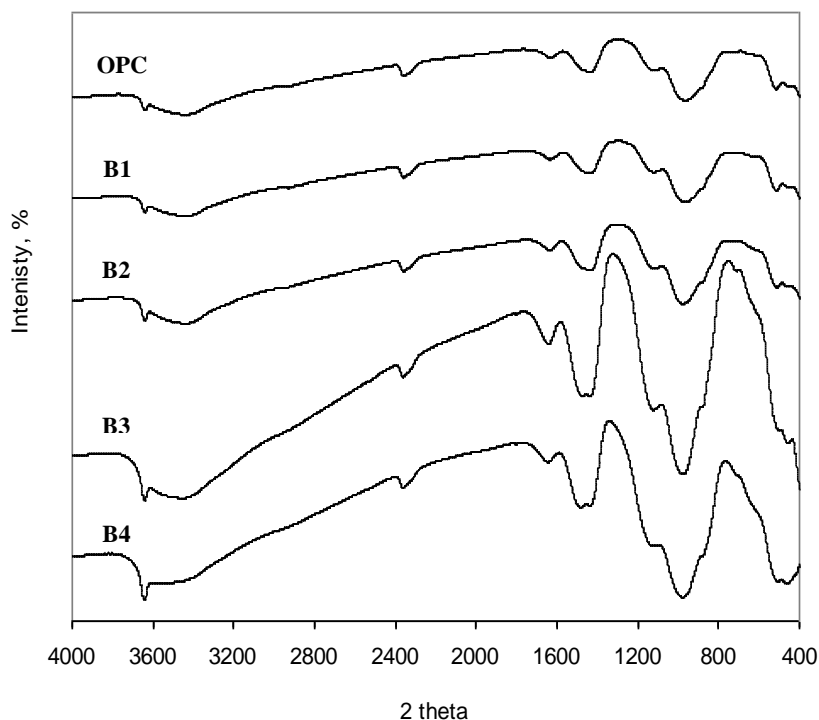


**Fig. 8.** The FTIR patterns of bagasse ash blended cements hydrated for 90 days.

Figure 9 shows the SEM micrographs of OPC and blended cement paste containing 15 % bagasse ash hydrated at 28 days. The SEM results illustrate the formation of hydration products C-S-H and CH which fill some pores of hydrated OPC paste. In case of bagasse ash blended cement paste, excess

bagasse ash forms a coating layer around anhydrous cement grains, hence, the degree of hydration and formation of hydration products decrease and as a result the total porosity of bagasse ash blended cement paste increases.

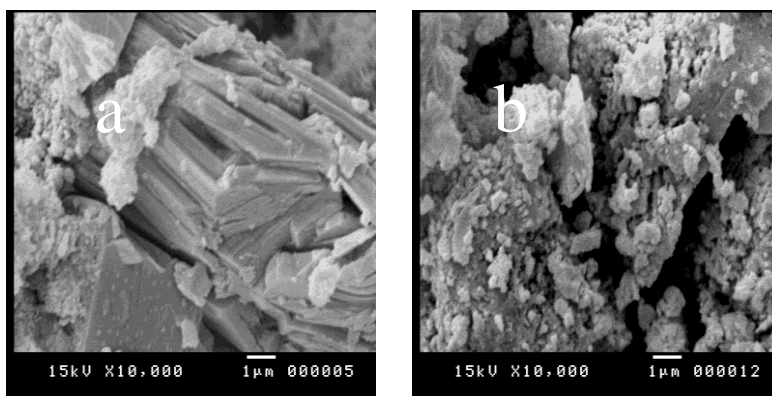


Fig. 9. SEM micrographs of (a) OPC and (b) B2 hydrated for 28 days.

#### *Cement immobilization of chromium (VI)*

Figure 10 and Table 7 illustrate the initial and final setting times of bagasse ash blended cement pastes hydrated with 5%  $K_2CrO_4$  solution. The water to cement ratio used is the same as in the hydration course. The setting time of OPC paste hydrated with 5%  $K_2CrO_4$  solution is longer than that hydrated with water due to that addition of Cr (VI) increases the setting times of cement<sup>(2,28)</sup>. The setting times of bagasse ash blended cement pastes hydrated with 5%  $K_2CrO_4$  solution are shorter than those hydrated with water due to that the incorporation of pozzolana may improve the hydration of cement in presence of Cr (VI) as well due to that addition of Cr (VI) may accelerate hydration reactions in presence of pozzolana due to precipitation of calcium chromate and the increased demand for  $Ca^{2+}$  ions in the cement pore solution. As a result, unhydrated cement fractions satisfy the increased demand of  $Ca^{2+}$  ions and accelerate hydration of  $C_3S$ <sup>(32,33)</sup>. The setting times elongate with bagasse ash content may be due to increasing the amount of mixing water, decreasing clinker content as well as the formation of a layer of bagasse ash particles around anhydrous cement grains which delays the hydration of  $C_3S$ .

Figure 11 and Table 8 illustrate the combined water content of bagasse ash blended cement pastes hydrated with 5%  $K_2CrO_4$  solution. The combined water content of bagasse ash blended cement pastes hydrated with 5%  $K_2CrO_4$  solution is higher than those hydrated with water due to that addition of Cr (VI) may accelerate hydration reactions due to precipitation of calcium chromate and the increased demand for  $Ca^{2+}$  ions in the cement pore solution. Unhydrated cement fractions satisfy the increased demand of  $Ca^{2+}$  ions and accelerate hydration of  $C_3S$ . The combined water content decreases with bagasse ash content due to that increasing bagasse ash content makes a dilution effect.

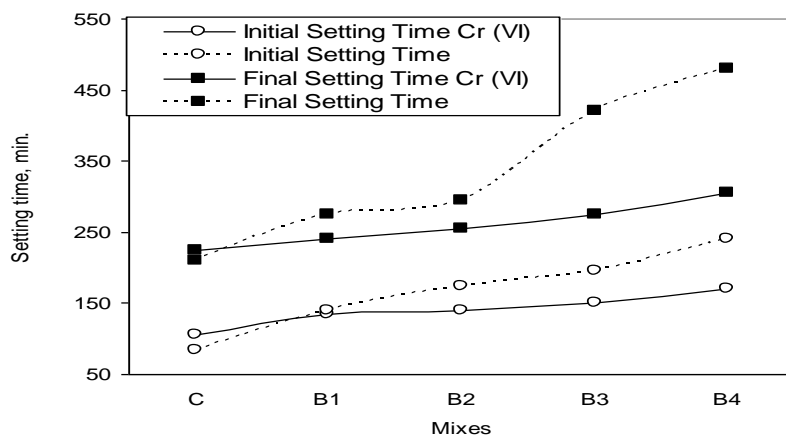


Fig. 10. The water of consistency, initial and final setting times of bagasse ash blended cement pastes hydrated with 5%  $K_2CrO_4$  solution.

TABLE 7. The initial and final setting times of bagasse ash blended cement pastes hydrated with 5%  $K_2CrO_4$  solution.

Sample	Initial setting time, min	Final setting time, min
C	105	225
B1	135	240
B2	140	255
B3	150	275
B4	170	305

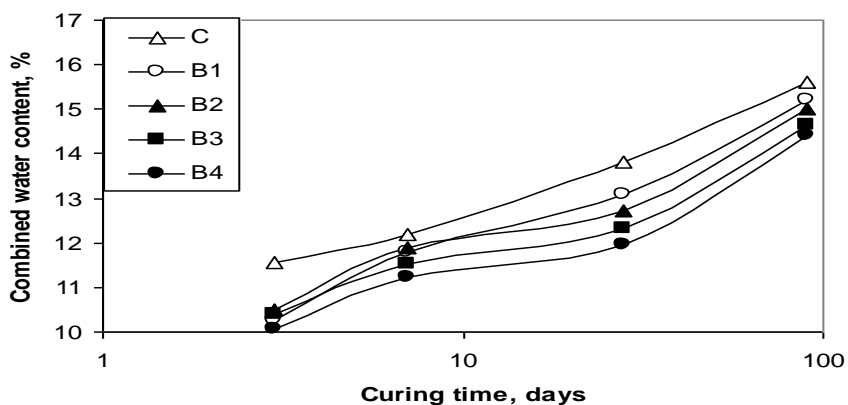
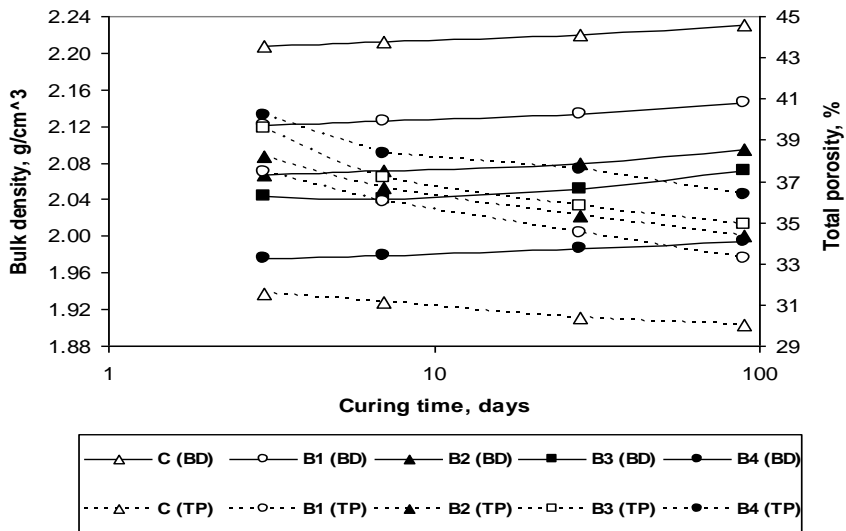


Fig. 11. The combined water content of bagasse ash blended cement pastes hydrated with 5%  $K_2CrO_4$  solution.

**TABLE 8.** The combined water content of bagasse ash blended cement pastes hydrated with 5%  $K_2CrO_4$  solution.

Sample	Combined water content, %			
	3 days	7 days	28 days	90 days
C	11.55	12.19	13.81	15.61
B1	10.25	11.80	13.10	15.22
B2	10.51	11.90	12.73	15.01
B3	10.40	11.53	12.32	14.66
B4	10.08	11.22	11.95	14.40

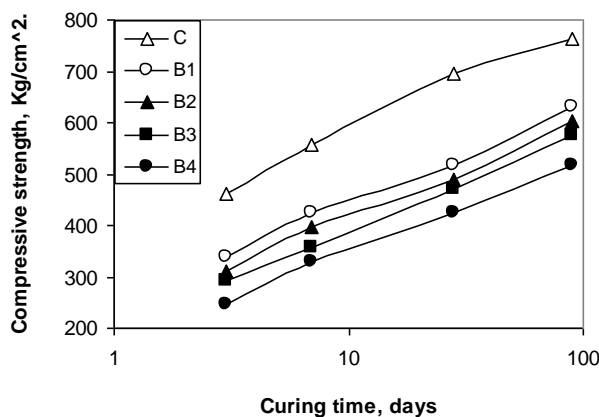
Figure 12 and Table 9 represent the bulk density and total porosity of bagasse ash blended cement pastes hydrated with 5%  $K_2CrO_4$  solution. The bulk density of bagasse ash blended cement pastes hydrated with 5%  $K_2CrO_4$  solution is lower than those hydrated with water because chromium addition affects the pore formation mechanism<sup>(22, 23)</sup> causing a wide variety of pore diameters hence the bulk density of cement pastes hydrated with  $K_2CrO_4$  solutions decreases. The total porosity of bagasse ash blended cement pastes hydrated with  $K_2CrO_4$  solutions is lower than those hydrated with water due to formation of calcium chromate precipitate which fills some of the open pores in hydrated cement pastes hence the total porosity decreases. The bulk density decreases while the total porosity increases with bagasse ash content due to that bagasse ash makes a dilution effect and have lower specific gravity.

**Fig. 12.** The bulk density and total porosity of bagasse ash blended cement pastes hydrated with 5%  $K_2CrO_4$  solution.

**TABLE 9.** The bulk density and total porosity of bagasse ash blended cement pastes hydrated with 5%  $K_2CrO_4$  solution.

Sample	Bulk density, g/cm <sup>3</sup>			
	3 days	7 days	28 days	90 days
C	2.2074	2.2123	2.2192	2.2314
B1	2.1212	2.1252	2.1336	2.1464
B2	2.0663	2.0712	2.0800	2.0955
B3	2.0437	2.0414	2.0521	2.0711
B4	1.9759	1.9789	1.9866	1.9950
Sample	Total porosity, %			
	3 days	7 days	28 days	90 days
C	31.52	31.10	30.39	30.05
B1	37.41	36.00	34.48	33.23
B2	38.22	36.72	35.30	34.33
B3	39.56	37.15	35.83	34.91
B4	40.21	38.32	37.61	36.38

Figure 13 and Table 10 represent the compressive strength of bagasse ash blended cement pastes hydrated with 5%  $K_2CrO_4$  solution. The compressive strength of bagasse ash blended cement pastes hydrated with 5%  $K_2CrO_4$  solution is lower than those hydrated with water because chromium addition affects the pore formation mechanism and reduces the compressive strength of the solidified cement especially at early ages. The compressive strength decreases with bagasse ash content because of the dilution effect of bagasse ash and the retardation effect of calcium chromate layer.

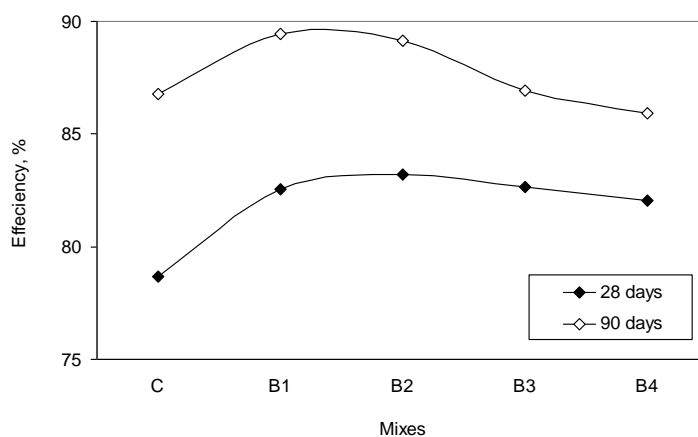
**Fig. 13.** The compressive strength of bagasse ash blended cement pastes hydrated with 5%  $K_2CrO_4$  solution.



**TABLE 10.** The compressive strength of bagasse ash blended cement pastes hydrated with 5%  $K_2CrO_4$  solution.

Sample	Compressive strength, Kg/cm <sup>2</sup>			
	3 days	7 days	28 days	90 days
C	461	556	697	763
B1	339	424	518	631
B2	311	395	490	603
B3	292	358	471	574
B4	247	330	424	518

Figure 14 and Table 11 represent the efficiency of Cr (VI) immobilization of bagasse ash blended cement pastes hydrated with 5%  $K_2CrO_4$  solution. The efficiency of Cr (VI) immobilization increases with bagasse content up to 15% bagasse ash content then decreases with further bagasse ash addition. The incorporation of bagasse ash may improve the hydration of cement in presence of Cr (VI) as well due to that addition of Cr (VI) may accelerate hydration reactions in presence of bagasse ash due to precipitation of calcium chromate which accelerates hydration of  $C_3S$ . The efficiency of Cr (VI) immobilization decreases with bagasse ash content because bagasse ash enhances the water demands of hydrated cement pastes, decreases clinker content as well as leading to formation of a layer of bagasse ash particles around anhydrous cement grains which delays the hydration of  $C_3S$ .

**Fig. 14.** The efficiency of Cr (VI) immobilization of bagasse ash blended cement pastes hydrated with 5%  $K_2CrO_4$  solution.

**TABLE 11. The efficiency of Cr (VI) immobilization of bagasse ash blended cement pastes hydrated with 5% K<sub>2</sub>CrO<sub>4</sub> solution.**

Sample	Immobilization efficiency, %	
	28 days	90 days
C	78.68	86.78
B1	82.53	89.46
B2	83.23	89.17
B3	82.64	86.95
B4	82.06	85.91

Figure 15 illustrates the XRD patterns of bagasse ash blended cement pastes hydrated with 5% K<sub>2</sub>CrO<sub>4</sub> solution. It was observed that the immobilization of Cr (VI) by cement progress with bagasse ash content as indicated from decreasing the intensity of CaCrO<sub>4</sub> and untreated K<sub>2</sub>CrO<sub>4</sub> with time. The content of CaCrO<sub>4</sub> decreases with bagasse ash content may be due to dilution effect of bagasse ash which replaces part of OPC. Bagasse ash consumes part of portlandite by its pozzolanic activity, hence the alkalinity of hydrated cement pasts containing bagasse ash decreases. As a result, the rate of precipitation of CaCrO<sub>4</sub> decreases with bagasse ash content. The immobilization of Cr (VI) by cement progress with bagasse ash content may be due to that formation of additional C-S-H as a result of the pozzolanic activity of bagasse ash encapsulate Cr (VI) ions as detected from decreasing the content of K<sub>2</sub>CrO<sub>4</sub> as bagasse ash increases.

Figure 16 illustrates the FTIR patterns of bagasse ash blended cement pastes hydrated with 5% K<sub>2</sub>CrO<sub>4</sub> solution. C-S-H absorption bands at 978 and 1644 cm<sup>-1</sup> decrease with bagasse ash content due to that bagasse ash forms a coating layer around anhydrous cement grains reducing the rate of hydration of cement hence cement immobilization of Cr (VI) decreases with bagasse ash content.

Figure 17 shows the SEM micrographs of OPC and blended cement paste containing 15 % bagasse ash hydrated with 5 % K<sub>2</sub>CrO<sub>4</sub> cured for 28 days. The SEM results illustrate that immobilization of Cr (VI) in bagasse ash blended cement paste was improved because of the pozzolanic activity of bagasse ash which reacts with CH and refines the microstructure of hydrated cement paste.

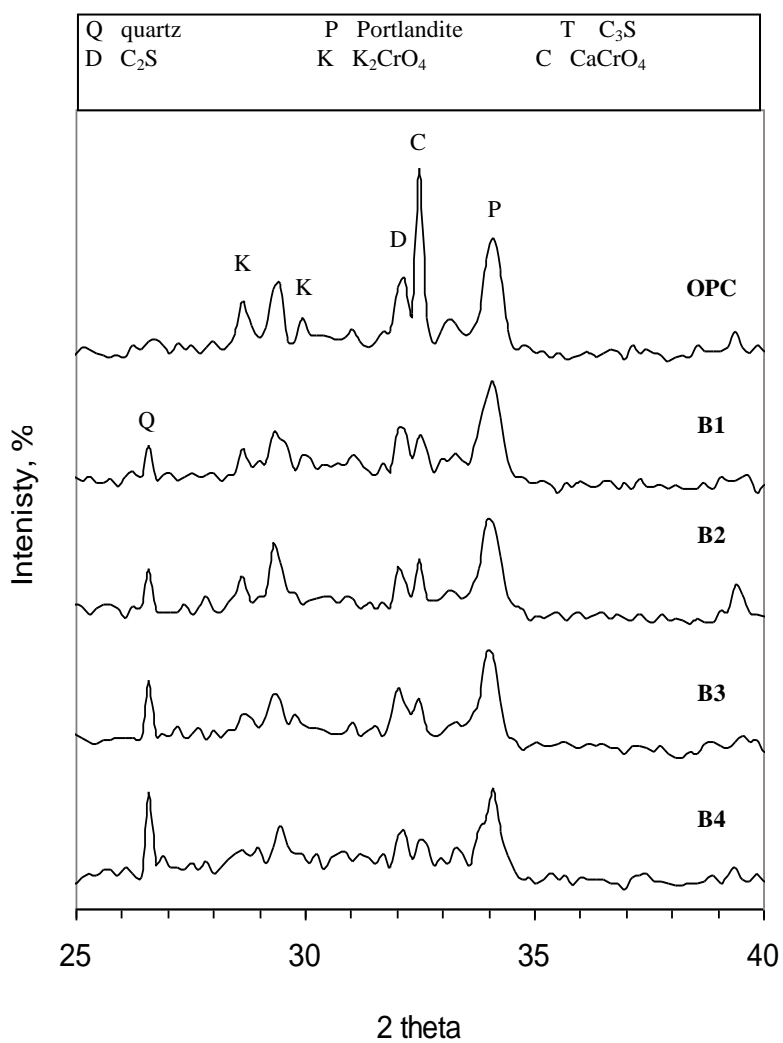


**Fig. 15.** The XRD patterns of bagasse ash blended cement pastes hydrated with 5% K<sub>2</sub>CrO<sub>4</sub> solution.

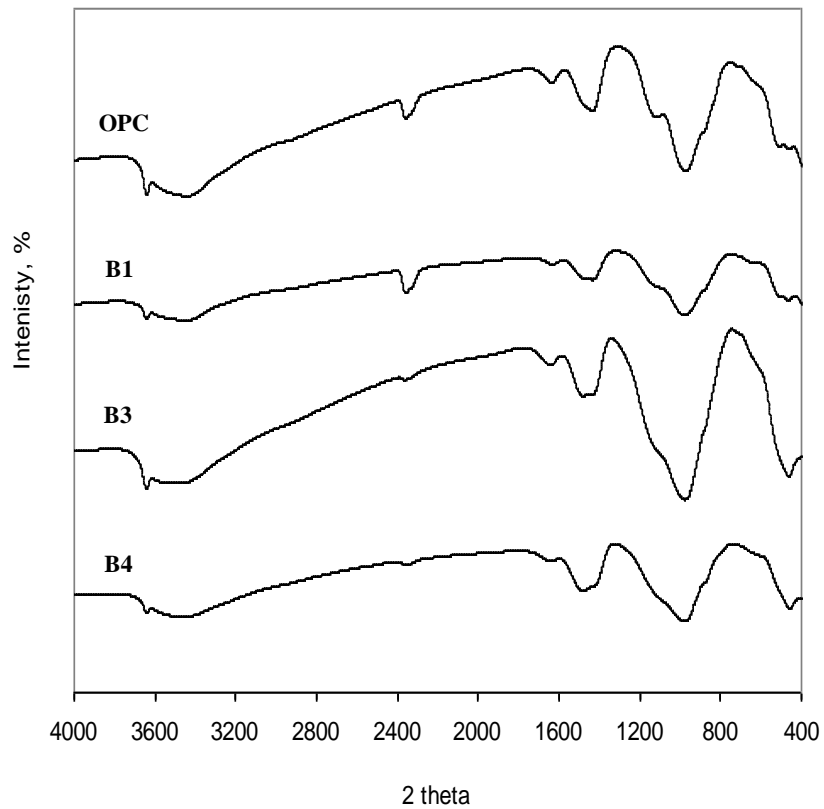


Fig. 16. The FTIR spectra of bagasse ash blended cement pastes hydrated with 5%  $K_2CrO_4$  solution.

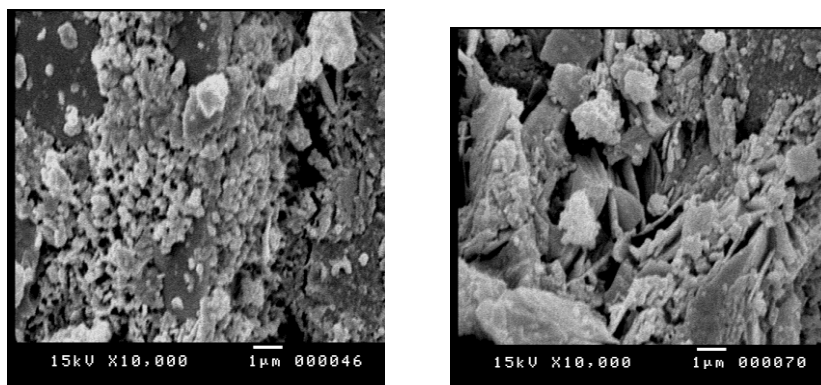


Fig. 17. SEM micrographs of (a) OPC and (b) B2 hydrated with 5%  $K_2CrO_4$  cured for 28 days.

### Conclusions

The main conclusions of this investigation are:

- 1- XRD, FTIR, TGA and SEM techniques illustrate that bagasse ash contains amorphous silica.
- 2- At the early ages of hydration, bagasse ash acts as a filler whereas at later ages it acts as pozzolana. Increasing bagasse ash content makes a dilution effect, require, higher water demands and forms a layer of bagasse ash particles around anhydrous cement grains which delays the hydration of cement.
- 3- The incorporation of up to 15% bagasse ash improves the hydration of cement in presence of Cr (VI) due to that addition of Cr (VI) may accelerate hydration reactions in presence of pozzolana due to precipitation of calcium chromate and the increased demand for  $\text{Ca}^{2+}$  ions in the cement pore solution. The situation is reversed with increasing bagasse ash content may be due to increasing the amount of mixing water, decreasing clinker content as well as the formation of a layer of bagasse ash particles around anhydrous cement grains which delays the hydration of cement.
- 4- According to this investigation, it was recommended that the blended cement which contains 15-20% bagasse ash can be used effectively for immobilization of concentrated waste Cr (VI) solutions ( $\approx 13000$  ppm Cr (VI)) after being mixed with the blended cement in a water to cement ratio of about 30%. The immobilized cement paste will set at about 4 hr and gain satisfactory compressive strength of about  $450 \text{ Kg/cm}^2$ . The immobilization efficiency will be more than 90% under this conditions.

### References

1. **Katz, S.A. and Salem, H.**, *"The Biological and Environmental Chemistry of Chromium"*, New York: VCH Publications (1994).
2. **Wang, S. and Vipulanandan, C.**, Solidification/stabilization of Cr (VI) with cement leachability and XRD analyses. *Cem. Concr. Res.* **30**, 385 (2000).
3. **Hasnain-Isa, M., Ibrahim, N. and Abdul-Aziz, H.**, Removal of chromium (VI) from aqueous solution using treated oil palm fibre. *J. Hazard. Mater.* **152**, 662 (2008).
4. **Bolto, B.A., Kotowski, M. and Pawlowski, L.**, Recovery of chromium from plating wastes. *Proceedings of Hazardous and Industrial Waste Management and Testing*, p. 278. (1984).
5. **Wiles, C.C.**, A review of solidification/stabilization technology. *J. Hazard. Mater.* **14**, 5 (1987)

6. **US EPA.**, "Treatment Technologies for Site Cleanup: Annual Status Report" (eleventh edition), EPA-542-R-03-009, February (2004).
7. **Umamaheswaran, K. and Batra, V.S.**, Physico-chemical characterization of Indian biomass ashes. *Fuel*, **87**, 628 (2008).
8. **Iyer, P.V.R., Rao, T.R. and Grover, P.D.**, "Biomass Thermo-Chemical Characterization", 3<sup>rd</sup> ed. IIT (Indian Institute of Technology), New Delhi (2002).
9. **Ali Jawaid, S.M. and Sheshank Raghatae**, Bagasse ash utilization in building industry. *Journal of Solid Waste Technology and Management*, **33** (4), p. 24 (2007).
10. **Suvimol, S. and Daungruedee, C.**, Bagasse ash: Effect of pozzolanic activity and application in cement use aspect. *The 3<sup>rd</sup> ACF International Conference-ACF/VCA*, pp. 165-173 (2008).
11. **Goyal, A. and Anwar, A.M.**, Poreproperties of sugarcane bagasse ash and its potential as cement - pozzolana binder", *12<sup>th</sup> International Colloquium on Structural and Geotechnical Engineering, 10-12 Dec. Cairo – Egypt* (2007).
12. **Siripairod, H. Polkert, S., Sujjavanich, S. and Chaysuwan, D.**, "Development of concrete flooring tiles by wastes, bagasse ash and fly ash for replacing type I Portland cement". *The 3<sup>rd</sup> ACF International Conference-ACF/VCA* (2008).
13. **Akram, T., Memon, S. A. and Obaid, H.**, Production of low cost self compacting concrete using bagasse ash, *Constr. Build. Mater.* **23**, 703 (2009).
14. **Banaag, V.F.E., Cañada, A.L.C., Meñes, M.O., Saldivar, K.Q. and Lo, D.S.**, Bagasse as an alternative aggregate in hollow CMU. *Symposium on Infrastructure Development and the Environment 2006, 7-8 December 2006, seameo-innotech, University of the Philippines, Diliman, Quezon City, philippines*.
15. **Singh, N.B., Singh, V.D. and Rai, S.**, Hydration of bagasse ash-blended Portland cement. *Cem. Conc.Res.* **30**, 1485 (2000).
16. **Stephan, D. A., Maleki, H., Knofel, D., Eber, B. and Hardlt, R.**, Influence of Cr, Ni and Zn on the properties of pure clinker phases: part II. C3A and C4AF. *Cem. Concr. Res.* **29**(5), 651 (1999).
17. **Stephan, D.B., Maleki, H., Knofel, D., Eber, B. and Hardlt, R.**, Influence of Cr, Ni and Zn on the properties of pure clinker phases: part I. C3A. *Cem. Concr. Res.* **29**(4), 545 (1999).
18. **Omotoso, O.E., Ivey, D.G. and Mikula, R.**, Quantitative X-ray diffraction analysis of chromium (III) doped tricalcium silicate pastes. *Cem. Concr. Res.* **26**(9), 1369 (1996)
19. **Park, C.K.**, Hydration and solidification of hazardous wastes containing heavy metals using modified cementitious materials. *Ceme. Concr. Res.* **30**(3), 429 (2000).

20. **Pera, J., Thevenim, G. and Chabannet, M.,** Design of a novel system allowing the selection of an adequate binder for solidification/stabilization of wastes. *Cem. Concr. Res.* **27**(10), 533 (1997).
21. **Trazza, M.A. and Ferraiuelo, M.F.,** Hydration study of limestone blended cement in the presence of hazardous wastes containing Cr (VI). *Cem. Concr. Res.* **33**, 1039 (2003).
22. **Chatterji, S.,** Mechanism of the  $\text{CaCl}_2$  attack on Portland cement concrete cement, *Cem. Concr. Res.* **8**, 461 (1978) .
23. **Goto, S. and Roy, D.,** Diffusion of ions through hardened cement pastes. *Cem. Concr. Res.* **11**, 757 (1981).
24. **Poon, C.S., Peters, D.J. and Perry, R.,** Mechanisms of metal stabilisation in cement based fixation processes. *Science of the Total Environment*, **41**, 55 (1985).
25. **Poon, C.S., Clark, A.I. and Perry, R.,** Permeability study of the cement based solidification process for the disposal of hazardous wastes. *Cem. Concr. Res.* **16**, 161 (1986).
26. **Tashiro, C. and Oba, J.,** The effect of  $\text{Cr}_2\text{O}_3$ ,  $\text{Cu}(\text{OH})_2$ ,  $\text{ZnO}$  and  $\text{PbO}$  on the compressive strength an hydrates of hardened C3A paste. *Cem. Concr. Res.* **9**, 253 (1979).
27. **Cannell, B.S., Eghmy, T.T. and Krzow, J.E.,** Heavy metal stabilisation in municipal solid waste combustion bottom ash using soluble phosphate. *Waste Manage.* **20**, 135 (2000).
28. **Neeraj, J. and Mridul, G.,** Effect of Cr(VI) on the hydration behavior of marble dust blended cement: Solidification, leachability and XRD analyses. *Constr. Build. Mater.* **22**, 1851 (2008).
29. **Rosetti, V. A. and Medici, F.,** Inertization of toxic metals in cement matrices: Effects on hydration, setting and hardening. *Cem. Concr. Res.* **25**, 1147 (1995).
30. **Tashiro, C., Takahashi, H., Kanaya, M., Hirakida, I. and Yoshida, R.,** Hardening property of cement mortar adding heavy metal compound and solubility of heavy metal from hardened mortar. *Cem. Concr. Res.* **7**, 283 (1977).
31. **Nocuh- Wczelik, W.,** Calorimetric studies of cementitious materials – chromium interactions. *Journal of Thermal Analysis*, **49**, 1147 (1997).
32. **Hills, C.D. and Pollard, S.J.T.,** Influence of interferences effect on the mechanical, microstructural and fixation characteristics of cement solidified hazardous waste forms. *J. Hazard. Mater.* **52**, 171 (1997).
33. **Crannel, B.S., Eighmy, T., Krzanowski, J.E., Eusdem, J.D., Shaw, E.L. and Francis, C.A.,** Heavy metal stabilization in municipal solid waste combustion bottom ash using soluble phosphate. *Waste Manage.* **20**, 135 (2000).

34. **Luz, C.A., Pera, J., Cheriaf, M. and Rocha, J.C.**, Behavior of calcium sulfoaluminate cement in presence of high concentrations of chromium salts. *Cem. Concr. Res.* **37**, 624 (2007).
35. **Glasser, F.P., Goumans, J.J.J., Van der Sleet, H. A. and Aalbers, Th. G.**, *Studies in Environmental Science*. Ed. Elsevier, Amsterdam, 77 (1994).
36. **Kindness, A. Macias and Glasser E. P.**, After E P. Glasser in J. J. J. Goumans, H. A. van der Sleet and Th. G. Aalbers, (Ed.) *Studies in Environmental Science*, Amsterdam, **77** (1994).
37. **Jacobs, J.H.**, Treatment and stabilization of a hexavalent chromium containing waste material. *J. Environ Prog.* **11**, 123 (1992).
38. **Vipulanandan, C. and Wang, S.**, Remediation of hexavalent chromium contaminated soil. *Proceedings of in-situ Remediation of the Geoenvironment*. ASCE, New York, 363 (1997).
39. **Salhan, A., Billingham, J. and King, A.C.**, The effect of a retarder on the early stages of the hydration of tricalcium silicate. *Journal of Engineering Mathematics*, **45** (3–4), 367 (2003).
40. **Tamas, F.D., Csetenyi, L. and Tritthart, E.**, Effect of adsorbent on the leachability of cement bonded electroplating wastes. *Cem. Conc. Res.* **22**, 399 (1992).
41. **Cheng, K.Y. and Bishop, P. L.**, Sorption, important in stabilised/solidified waste forms. *Hazardous Waste and Hazardous Materials*, **9**, 289 (1992).
42. **Ortego, J.D., Jackson, S. and Yu, G.S.**, Solidification of hazardous substances – a TGA and FTIR study of Portland cement containing metal nitrates. *Journal of Environmental Science and Health*, **A24**, 589 (1989).
43. **Frey, H.C., Herrera, E., Tittlebaum, M.E. and Yang, S.L.**, Immobilisation mechanisms in solidification/stabilisation of Cd and Pb salts using Portland cement. *Environ. Sci. Technol.* **24**, 867 (1990).
44. **Kitamura, M., Konno, H., Yasui, A. and Masuoka, H.**, Controlling factors and mechanism of reactive crystallisation of calcium carbonate polymorphs from calcium hydroxide suspensions. *Journal of Crystal Growth*, **236**, 332 (2002).
45. **Omotoso, O.E., Ivey, D.G. and Mikula, R.**, Hexavalent chromium in tricalcium silicate. *J. Mater. Sci.* **33**, 507 (1998).
46. **Macias, A., Kindness, A. and Glasser, F.P.**, Impact of carbon dioxide on the immobilization potential of cemented wastes: chromium. *Cem. Concr. Res.* **27**, 215 (1997).
47. **Schwiete, H.E. and Ludwig, U.**, Crystal structures and properties of cement hydration products (hydrated calcium aluminates and ferrites). Hydration of Cements. *Proceedings of the Fifth International Symposium on the Chemistry of Cement*, II, **37**, (1968).



48. **Kumarathasan, P., McCarthy, G.J., Hassett, D.J. and Pflughoeft-Hassett, D.F.**, Oxyanion substituted ettringites: synthesis and characterization; and their potential role in immobilization of As, B, Cr, Se, and V. Fly Ash and Coal Conversion By-Products: Characterization, Utilization, and Disposal II, Materials. *Research Society Symposium Proceedings*, **178**, 83 (1990)
49. **Bensted, J. and Varma, S.P.**, Ettringite and its derivatives. II. Chromate substitution. *Silicates Ind.* **37**, 315 (1972).
50. **Dermatas, D. and Meng, X.**, Utilization of fly ash for stabilization/solidification of heavy metal containing soils. *Engineering Geology*, **70**(3-4), 377 (2003).
51. **Dermatas, D. and Moon, D.H.**, Chromium leaching and immobilization in treated soils. *Environmental Engineering Science*, **23**(1), 77 (2006).
52. **Akhter, H., Butler, L.G., Branz, S., Cartledge, F.K. and Tittlebaum, M.E.**, Immobilization of As, Cd, Cr and Pb-containing soils by using cement or pozzolanic fixing agents. *J. Hazard Mater.* **24**, 145 (1990).
53. **Albino, V., Cioffi, R., Santoro, L. and Valenti, G. L.**, Stabilization of residue containing heavy metals by means of matrices generating calcium trisulphoaluminate and silicate hydrates. *Waste Manage. Res.* **14**, 29 (1996).
54. **Cheryl E., Halim, Rose Amal, Donia Beydoun, Jason A. Scott, Gary Low,** Implications of the structure of cementitious wastes containing Pb(II), Cd(II), As(V), and Cr(VI) on the leaching of metals. *Cem. Concr. Res.* **34**, 1093 (2004).
55. **Qijun, Yu.T., Nagataki, S., Jinmei, L., Saeki, T. and Hisada, M.**, The leachability of heavy metals in hardened fly ash cement and cement-solidified fly ash. *Cem. Concr. Res.* **35**, 1056 (2005).
56. **Pinto, C.A., Hamassaki, L.T., Valenzuela-Diaz, F.R., Dweck, J. and Büchler, P.M.**, Tannery waste solidification and stabilization thermal and mechanical characterization. *Journal of Thermal Analysis and Calorimetry*, **77**, 777 (2004).
57. **El-Roudi, A.M., Tantawy, M.A. and Salim, A.A.**, Thermal treatment and pozzolanic activity of bagasse ash waste, directed for publication in cement and concrete composites. *Cement and Concrete Composite* (under publication)
58. **ASTM Designation: C 187-98**, "Standard Test Method for normal consistency of hydraulic cement", *Annual Book of ASTM Standards*, 04.01 (2002).
59. **ASTM Designation: C 191-01a**, "Standard Test Method for time of setting of hydraulic cement by Vicat needle", *Annual Book of ASTM Standards*, 04.01 (2002).
60. **Gennaro, R., Cappelletti, P., Cerri, G., Gennaro, M., Dondi, M. and Langella, A.**, Zeolitic tuffs as raw materials for lightweight aggregates. *Appl. Clay Sci.* **25**, 71 (2004).
61. **ASTM Designation: C109-80**, "Standard Test Methods for compressive strength of hydraulic cements", *ASTM Standards* (1983).

62. **Pavlik, J., Tydlit, V., Cerny, R., Klecka, T., Bouska, P. and Rovnanikova, P.,** Application of a microwave impulse technique to the measurement of free water content in early hydration stages of cement paste. *Cem. Concr. Res.* **33**, 93 (2003).
63. **Copeland, L.E. and Hayes, T.C.,** Porosity of hardened Portland cement pastes. *ACI Mater. J.* **27**, 633 (1956).
64. **USEPA.,** *Method 1311: toxicity characteristic leaching procedure*, In EPA SW-846: test methods for evaluating solid waste, physical/chemical methods, July (1992).
65. **Gupta, V.K., Jain, C.K., Ali, I., Sharma, M. and Sainia, V.K.,** Removal of cadmium and nickel from wastewater using bagasse fly ash-a sugar industry waste. *Water Res.* **37**, 4038 (2003).
66. **ASTM Designation: C 618-89,** "Standard specification for coal fly ash and raw or calcined natural pozzolana for use as a mineral admixture in concrete", *ASTM Standards* (1998).
67. **EI-Didamony, H., Helmy, I.M., Amer, A.A. and Heikal, M.,** Utilization of Egyptian by-products in the preparation of blended cements. *Zement-Kalk-Gips*, **48** (9), 502 (1995).
68. **Hwang, C.L. and Shen, D.H.,** The effect of blast furnace slag and fly ash on the hydration of Portland cement. *Cem. Concr. Res.* **21**, 410 (1991).
69. **Khandaker, M. and Hossain, A.,** Properties of volcanic pumice based cement and lightweight concrete. *Cem. Concr. Res.* **34**, 283(2004).
70. **Yogendran, V., Langan, B.W. and Ward, M.A.,** Hydration of cement silica fume paste. *Cem. Concr. Res.* **21**, 691 (1991).

(Received 15/9/2011;  
accepted 19/10/2011)

### دفع الكروم السداسى فى عجائن الاسمنت المخلوط برماد الباجاس

احمد محمد الروضى ، محمد احمد طنطاوى و علاء احمد على سالم  
قسم الكيمياء - كلية العلوم - جامعة المنيا - المنيا - مصر .

الهدف من هذا العمل هو دراسة إمكانية الاستفادة من رماد الباجاس في تحسين تصلب/تثبيت الكروم السداسى في عجائن الاسمنت . طبقاً للنتائج توصي هذه الدراسة بإمكانية استخدام الاسمنت المخلوط الذي يحتوي على ١٥-٢٠ ٪ من رماد الباجاس بفعالية في تصلب/تثبيت الملوثات المحتوية على تركيزات من الكروم السداسى (≈ ١٣٠٠٠ جزء في المليون) بعد خلطها مع الاسمنت المخلوط باستخدام نسبة ماء/اسمنت حوالي ٣٠ ٪ . تتصلب عينة الاسمنت في أقل من ٤ ساعات وتكتسب قوة تحمل ميكانيكي مرضية لا تقل عن ٤٥٠ كيلو جرام/سم<sup>٢</sup> وفعالية احتواء الاسمنت للكروم السداسى لا تقل عن ٩٠ ٪ تحت هذه الظروف .